International Journal of Electrical and Electronics Engineering Research (IJEEER)
ISSN(P): 2250-155X; ISSN(O): 2278-943X
Vol. 3, Issue 5, Dec 2013, 81-88

ELECTRON IMPACT IONIZATION OF HYDROGENLIKE SYSTEMS

M. K. ALAM[1], M. A. RAHMAN[2] & M. R. TALUKDER[3]

[1]Department of Physics, Pabna University of Science and Technology, Pabna, Bangladesh

[2,3]Department of Applied Physics and Electronic Engineering, University of Rajshahi, Bangladesh

ABSTRACT

The electron impact single ionization cross sections, of hydrogen like H, He^{+}, Li^{2+}, B^{4+}, C^{5+}, N^{6+}, O^{7+}, Ne^{9+}, Ar^{+17}, Fe^{25+}, Mo^{41+}, Dy^{65+}, Au^{78+}, Bi^{82+}, and U^{91+} targets with the atomic number $Z = 1-92$ and the incident electron energies from threshold to about $10^6\ eV$, are calculated using a modified version of the recently propounded simplified Bell (SBELL) model [M.R. Talukder, S. Bose, M.A.R. Patoary, A.K.F. Haque, M.A. Uddin, A.K. Basak, M. Kando, Eur. Phys. J. D 46, 281(2008)]. The results of the present analysis are compared with the available experimental results and theoretical calculations. The proposed model calculates reasonably accurate cross sections for any hydrogen like targets from H-U. This model may be a prudent selection for the application in applied sciences due to its simple inherent structure.

KEYWORDS: Single Ionization, Electron Impact Ionization, Cross Section, Hydrogen-Like

INTRODUCTION

Electron impact collision processes are used in different fields [1] of applied and fundamental researches. There are several quantum mechanical models [2-8] are anticipated to determine electron impact single ionization (EISI) cross sections for atomic and ionic targets. The quantum mechanical models are capable of calculating differential ionization and total single ionization cross sections solving Schrödinger equation. The quantum mechanical convergent close coupling, distorted wave Born approximation (DWBA) and R-matrix methods are very often used to determine EISI cross sections. However, quantum as well as experimental method provides cross sections at discrete energies and preferred targets. In addition, quantum method requires huge computation resources and time. Moreover, this method incapable of providing user-friendly cross-sections as expected by the applied researchers. This constraint can be overcome by the analytic model. Hence, it is necessary a reliable but simple analytic model that can calculate EISI cross section for the applied researchers.

There are several empirical, semi-empirical, classical, and semi-classical formulae are proposed and reviewed [9-25]. The models of Lotz [15,16], Deutsch-Mark (DM) [10], binary-encounter-dipole (BED) model [19] and modified Bell (BELI) [17] models are extensively used for the estimation EISI cross sections. DM and BED models are used to estimate and represent cross sections of a few atoms, ions and molecules. On the other hand, the MRIBED (modified relativistic BED [20]) model determines EISI cross sections for selected species. There are several empirical models are propounded [17] for the calculation of cross sections without generalization of model parameters. A semi-classical model [22] produces inaccurate cross sections in most cases and valid for atoms and ions. Besides, simple empirical models [23,25] are anticipated, which are applicable either for very selected targets or in many cases applicable to low incident energies. The above constraints motivated us to determine adequate EISI cross sections for diverse targets and wide range of incident energies that may contribute to fill up, to some extent, the gap between the available cross sections data and the demand level. In order to fill up the gap, Talukder et al. [24] anticipated a simplified Bell *et al.* [18], here after will be called SBELL, model to increase the competence and to decrease the number of fitting parameters and used with incredible

success to the description of EISI cross sections for neutral targets from $Z = 1-92$. It may be of interest to explore the SBELL model to ionic targets incorporating ionic correction factor with it. The model so framed is, hereafter, will be referred to as the modified (SBELL) MSBELL model.

The EISI cross sections of hydrogenic isoelectronic H, He^{+}, Li^{2+}, B^{4+}, C^{5+}, N^{6+}, O^{7+}, Ne^{9+}, Ar^{+17}, Fe^{25+}, Mo^{41+}, Dy^{65+}, Au^{78+}, Bi^{82+}, and U^{91+} sequence have been estimated using the presented MSBELL model. The predicted EISI cross sections of the MSBELL model have been compared with the available experimental and other theoretical calculations.

This paper is frame as follows. The outline of the MSBELL model is sketched in Section 2. In Section 3, we discuss the results of MSBELL in comparison with the experimental results and theoretical calculations. Section 4 is devoted to the discussion of the results and the conclusions arrived at.

OUTLINE OF THE MODEL

Bell *et al.* [18] proposed a semi-empirical formula, known as the BELI form [17], for fitting the EISI cross sections of atoms and ions. The formula is of the form

$$\sigma_{BELI}(E) = \frac{1}{EI}\left\{ A\ln(E/I) + \sum_{k=1}^{N} B_k (1 - I/E)^k \right\}. \qquad (1)$$

Here, E is the kinetic energy of the incident electron, I is the ionization potential, and A and B_k are the fitting coefficients.

Talukder et al. [24] proposed an empirical model to improve the efficiency and to reduce the number of fitting coefficients of the BELI model [17] for the description of EISI cross sections to cover the wide range of neutral targets from $Z = 1-92$. The EISI cross section is given [24] as

$$\sigma_{SBELL}(E) = \sum_{nl} \frac{N_{nl} I_{nl}}{E} \{ A_{nl} \ln(E/I_{nl}) + B_{nl}(1 - I_{nl}/E) \}, \qquad (2)$$

where A_{nl} and B_{nl} are the fitting parameters expressed as the function of normalized potential U_R. I_{nl} is the ionization potential of the ionizing nl orbit. E and I_{nl} both are expressed in eV. N_{nl} is the number of electrons in the ionizing nl orbit. The parameter A_{nl} is the Bethe coefficient and determines the high energy behavior of the cross section. Here the summation is over the orbit nl of the target. It is noted that one can neglect summation symbol for hydrogen isoelectronic sequence because the targets have only $1s$ orbital, considered herein. Eq. (2) contains two orbital dependent parameters A_{nl} and B_{nl}. This formula also ensures the correct behavior of the cross sections at both low and high impact energies. However, Eq. (2) is modified by incorporating in it the ionic correction factor to extend the applicability of SBELL model for ionic targets. As it is well known that the ionic effect decreases with the increase of the incident electron energy. In light of this fact, we suggest an ionic correction [26] in the form of a multiplying factor F_I

$$F_I = 1 + n\left(\frac{q}{ZU_R}\right)^{\lambda}, \qquad (3)$$

where n and λ are fitting parameters. The optimum values obtained for n and λ, as will be discussed later, are $n = 1.5$ and $\lambda = 0.5$.

Finally, the proposed MSBELL model for the description of EISI cross section σ_{MSBELL} is given by

$$\sigma_{MSBELL} = F_I \sigma_{SBELL}(E). \qquad (4)$$

In Eq. (4), the fitting parameters A_{nl} and B_{nl} are generalized by making them dependent on I_{nl}. The parameters A_{nl} and B_{nl} are expressed as

- for $1 \le U_R \le 100$

$$A_{nl} = \frac{1.44 \times 10^{-10} U_R}{(1 + 69U_R)^{3.08}}, \qquad (5a)$$

$$B_{nl} = -\frac{1.72 \times 10^{-10} U_R}{(1 + 69U_R)^{3.15}}, \qquad (5b)$$

- (b) $100 \le U_R \le 10^4$

$$A_{nl} = \frac{2.38 \times 10^{-11} U_R}{(1 + 69U_R)^{2.90}}, \qquad (5c)$$

$$B_{nl} = -\frac{2.11 \times 10^{-11} U_R}{(1 + 69U_R)^{2.94}}, \qquad (5d)$$

Ionization potential is normalized by $U_R = I_{nl} / R$, where R is the Rydberg energy. The units of A_{nl} and B_{nl} are expressed in cm^2.

RESULTS AND DISCUSSIONS

We have used the published results for ionization potentials of neutral targets given by Desclaux [27]. On the other hand, the ionization potentials for the ionic targets are calculated using Dirac-Hartree-Fock code [28]. Using the MSBELL model we have calculated EISI cross sections for the hydrogen isoelectronic sequence, using Eq. (4) along with Eqs. (5), over a wide incident electron energies from threshold to $10^6\ eV$. The results presented here only for H, He^+, Li^{2+}, B^{4+}, C^{5+}, N^{6+}, O^{7+}, Ne^{9+}, Ar^{+17}, Fe^{25+}, Mo^{41+}, Dy^{65+}, Au^{78+}, Bi^{82+}, and U^{91+} targets whose either experimental or theoretical results are available. Most recent experimental as well as theoretical results are taken into account to compare the results obtained by the MSBELL model. It is interesting to note that this model can be used for the description of EISI cross sections for any hydrogen-like target from H to U.

The ionic correction factor F_I in Eq. (3) with the parameter values $n = 1.5$ and $\lambda = 0.5$ are optimized in such a way for which Eq. (4) describes the best EISI cross sections with respect to the experimental data for the range of

incident energies and for the targets considered herein. The coefficients of the parameters A_{nl} and B_{nl} in Eqs. (5a) – (5d) are determined from the overall best fits of our predicted cross sections to the experimental results. A measure of the quality of best fit is obtained by minimizing the chi-square defined by

$$\chi^2 = \sum_i \left[\frac{\sigma_c(E_i) - \sigma_x(E_i)}{\sigma_x(E_i)} \right]^2,$$

where $\sigma_c(E_i)$ and $\sigma_x(E_i)$ refer, respectively, to the theoretical and experimental cross sections at the energy point E_i. The optimum values of the coefficients, in terms of which the parameters A_{nl} and B_{nl} are defined, are obtained using a non-linear least-square fitting program.

In the figures, open- and filled symbols represent, respectively, the quantum and experimental results. On the other hand, thick continuous line represents the prediction by the proposed model while the dashed lines are the prediction by classical, semi-classical, or empirical formula.

Figures 1(a-c) show the EISI cross sections of H, He^+, and Li^{2+}, respectively. The MSBELL predictions for H are displayed in Figure 1(a), along with the experimental cross sections [29] and the results of TPDW01 (relativistic two-potential distorted-wave approximation [30]), MRIBED [31], and DM [10] theories. The TPDW01 and DM results largely over estimate the experimental results over the wide incident energies. The MSBELL and MRIBED calculations are almost identical and agree well with the experimental findings. In Figure 1(b), we present the calculated cross sections for He^+, experimental results [32], and findings from the TPDW01 [30], DM [10], and MRIBED [31] theories. A little discrepancy is found with MSBELL calculations and the experimental results in the peak region but the MSBELL and TPDW01 results agree well. MSBELL predictions for Li^{2+} are depicted, in Figure 1(c), along with the experimental cross sections [33] and the FRDWBA (fully relativistic DWBA [34]), MRIBED [31], DM [10], and DWBA [35] results. The MRIBED calculations slightly underestimate from 200-600eV while FRDWBA results overestimate the experimental results after 3keV. Theoretical results of DM, DWBA, MRIBED, and MSBELL are almost identical. However, comparisons among the experimental and theoretical findings dictate that the MSBELL calculation is the best.

Figures 2(a-c) show the EISI cross sections of B^{4+}, C^{5+} and N^{6+}, respectively. The MSBELL predictions for B^{4+} are displayed, in Figure 2(a), along with the experimental results [36], and the theoretical FRDWBA [34], DWBA [35], and MRIBED [31] findings. The predictions from the MSBELL theory are completely identical, and excellent agreements are found with the experimental results over the wide incident energies. The MSBELL model is definitely doing the best than FRDWBA, DWBA, and MRIBED models. In Figure 2(b), we present the calculated cross sections for C^{5+}, experimental results [36,37], and theoretical findings from DWBA [35], TPDW01 [30], and MRIBED [31]. All theoretical calculations, except that of MRIBED from peak to high incident energies, are identical with the experimental results. Among all the theories, the best agreement is found between the experimental [36] and MSBELL results over the wide incident energies. The MSBELL predictions for N^{6+} are depicted, in Figure 2(c), along with the experimental cross sections [36,37] and the theoretical FRDWBA [34], DWBA [35], MRIBED [31], and DM [10] findings. In this case also, the MSBELL predictions agree completely with the experimental results [36] over the domain of incident energies. Since, the MSBELL predictions are completely successful for the description of EISI cross sections for B^{4+}, C^{5+} and N^{6+} targets over incident energies considered herein than the theoretical findings of FRDWBA, DWBA, TPDW01 and MRIBED.

In Figures 3(a-c), we compare the MSBELL predictions for the EISI cross sections of O^{7+}, Ne^{9+}, and Ar^{17+} targets, respectively, with the experimental cross sections [36,37]. The other theoretical calculations used for comparison in these figures are DWBA [35], FRDWBA [34], MRIBED [31], of Kunc [38], and DWBE (distorted-wave Born exchange [39]). The MSBELL and DWBA results agree well with the experimental measurements, as seen in Figure 3(a) for O^{7+}. The DM and MRIBED calculations slightly underestimate the experimental results in the low energy region while slightly overestimate from peak to high energy region. Since, the prediction of MSBELL is the best than that of DM and MRIBED calculations. In Figure 3(b), both the MSBELL and DM calculations underestimate the experimental results in the peak region. But the agreement of experimental measurement is much better for MSBELL than DM calculations. However, in case of Ar^{17+} as shown in Figure 3(c), excellent agreement is found with the experimental results as well as with the DWBE calculations. Since, it is evident that successfulness of the MSBELL predictions is much higher than those of other theoretical calculations for the description of EISI cross sections for O^{7+}, Ne^{9+}, and Ar^{17+} targets over incident energies considered herein.

Figures 4(a-c) illustrate the EISI cross sections of Fe^{25+}, Mo^{41+}, and Dy^{65+}, respectively. The MSBELL calculations for Fe^{25+} are displayed in Figure 4(a), along with the experimental cross sections [40] and the results of FRDWBA [34], and O'Rourke [41] theories. The MSBELL and FRDWBA calculations are identical and fairly good agreements of MSBELL predictions with the experimental results are found within the experimental error. In Figure 4(b), we present the calculated MSBELL cross sections of Mo^{41+}, experimental results [40,42], and theoretical findings from the DWBA [35], and FRDWBA [34]. The DWBA and MSBELL calculations are identical in pattern, but the DWBA calculations slightly underestimate the experimental results while a better agreement is found for the MSBELL results within the experimental error. The MSBELL predictions of Dy^{65+} are depicted, in Figure 4(c), along with the experimental cross sections [38] and the theoretical FRDWBA [34], DWBA [35], RDWBA [43] and MRIBED [31] findings. Fairly good agreement is found between the MSBELL predictions and the experimental results [40]. As a whole, the MSBELL predictions are successful for the description of EISI cross sections for Fe^{25+}, Mo^{41+}, and Dy^{65+} targets over the incident energies considered herein than the theoretical findings of FRDWBA, DWBA, RDWBA, and MRIBED.

Figures 5(a-c) display the MSBELL calculations for Au^{78+}, Bi^{82+}, and U^{91+}. In Figure 5(a), we compare the experimental EISI cross sections [44], along with the findings of FRDWBA [34], and RDWBA [43] theories. The MSBELL calculations slightly overestimate the experimental results, but the pattern is identical with respect to the FRDWBA, and RDWBA calculations. The MSBELL predictions are, depicted in Figure 5(b) for Bi^{82+}, compared with the experimental findings [44], along with the results of DWBA [35], and MRIBED [31] theories. The DWBA calculations slightly underestimate the experimental measurements over the incident energies considered herein. The MRIBED results increase with the increase of incident energy due to the inclusion of relativistic effect in their model. An identical pattern is observed between the DWBA and MSBELL results over the domain of incident energies. However, an excellent agreement is found between the MSBELL calculations and the experimental results. Figure 5(c) compares the MSBELL findings with the experimental results [44] together with the TPDW01 [30], RDWBA [43], DWBA [35], and FRDWBA [34] calculations, for U^{91+}. Calculations of TPDW01, RDWBA, and FRDWBA theories underestimate the experimental results over the wide incident energies. The MSBELL results agree well with the experimental finding and the DWBA calculations. Cross sections, calculated by the MRIBED and DWBA theories, increase with the increase of incident energy due to the influence of relativistic effect. Finally, the MSBELL calculations successfully, with respect to the other theoretical results considered herein, describe the EISI cross sections for Au^{78+}, Bi^{82+}, and U^{91+} targets over the domain of incident energies.

CONCLUSIONS

The MSBELL model is seen to provide a good description of the experimental EISI cross section data for any hydrogen like targets with the atomic number $Z = 1 - 92$ and with the incident electron energies from threshold to $10^6\ eV$. In the description of the available experimental data with respect to the domain of species and incident energies, the level of performance of the present model seems to be the best or as good as the other sophisticated theoretical methods, like DWBA, TPDW01, FRDWBA, considered herein for comparison. It is demonstrated that the present MSBELL model provides very encouraging and reliable results for the EISI cross sections. In order to decide the predictive role of our model, it is our intention to extend this model to other, like He, Li, Be etc., system. However, the MSBELL model with its simple structure may turn out to be a very efficient alternative for the calculations of EISI cross sections for hydrogen like targets for the applications in applied sciences.

REFERENCES

1. M.R. Talukder, D. Korzec, M. Kando, J. Appl. Phys. 91 (2002) 9529.
2. M. Baertschy, T.N. Rescigno, C.W. McCurdy, Phys. Rev. A 64 (2001) 022709.
3. S. Jones, D.H. Madison, Phys. Rev. A 62 (2000) 042701.
4. D.V. Fursa, I. Bray, Phys. Rev. A 52 (1995) 1279.
5. D. Kato, S. Watanabe, Phys. Rev. Lett. 74 (1995) 2443.
6. J.C. Chang, H.L. Sun, W.Y. Cheng, K.N. Huang, Phys. Rev. A 69 (2004) 052713.
7. I. Bray, J. Phys. B 28 (1995) L247.
8. I. Bray, Phys. Rev. A 46 (1992) 6995.
9. S. M. Younger, T. D. Märk, in: T.D. Mark G.H. Dunn (Eds.), Electron Impact Ionization, Springer-Verlag, Berlin, 1985, p. 24.
10. H. Deutsch, T.D. Märk, Int. J. Mass Spect. Ion Proc. 79 (1987) R1.
11. H. Deutsch, K. Becker, S. Matt, T.D. Märk, Int. J. Mass Spect. 197 (2000) 37.
12. D. Margreiter, H.Deutsch, T.D.Märk, Int. J. Mass Spect. Ion Proc. 139(1994) 127.
13. H. Deutsch, K. Becker, T.D. Märk, Contrib. Plasma Phys. 35 (1995) 421.
14. H. Deutsch, K. Becker, B. Gstir, T.D. Märk, Int. J. Mass Spect. 213 (2002) 5.
15. W. Lotz, Z. Phys. 216 (1968) 241.
16. W. Lotz, Z. Phys. 232 (1970) 101.
17. A.L. Godunov and P.B. Ivanov, Phys. Scr. 59 (1999) 277.
18. K.L. Bell, H.B. Gilbody, J.G. Hughes, A.E. Kingston, F.J. Smith, J. Phys. Chem. Ref. Data 12 (1983) 891.
19. Y.-K. Kim, M.E. Rudd, Phys. Rev. A 50 (1994) 3954.
20. M.A. Uddin, A.K.F. Haque, A.K. Basak, K.R. Karim, B.C. Saha, Phys. Rev. A 72 (2005) 032715.

21. M.R. Talukder, S. Bose, S. Takamura, Int. J. Mass Spectrom. 269 (2008) 118.
22. M. S. Gryzinski, Phys. Rev. 138 (1965) 336.
23. V. A. Bernshtam, Y. V. Ralchenco, Y. Maron, J. Phys. B 33 (2000) 5025.
24. M.R. Talukder, S. Bose, M.A.R. Patoary, A.K.F. Haque, M.A. Uddin, A.K. Basak, M. Kando, Eur. Phys. J. D 46 (2008) 281.
25. Y.K. Kim, J.P. Desclaux, Phys. Rev. A 66 (2002) 012708.
26. C.J. Fontes, D.H. Sampson, H.L. Zhang, Phys. Rev. A 59 (1999) 1329.
27. J.P. Desclaux, At. Data Nucl. Data Tables 12 (1973) 325.
28. M.Y. Amusia, L.V. Chernysheva, Computations of Atomic Processes, Institute of Physics Publishing, Bristol, 1997.
29. M.B. Shah, D.S. Elliott, H.B. Gilbody, J. Phys. B 20 (1987) 3501.
30. T.Y. Kuo, C.J. Chen, S.W. Hsu, K.N. Huang, Phys. Rev. A 48 (1993) 4646.
31. M.A. Uddin, A.K.F. Haque, A.K. Basak, B.C. Saha, Phys. Rev. A 70 (2004) 032706.
32. B. Peart, K.T. Dolder, J. Phys. B 2 (1969) 1169.
33. K. Tinschert, A. Müller, G. Hoffmann, K. Hubert, R. Becker, D.C. Gregory, E. Salzborn, J. Phys. B 22 (1989) 531.
34. C.J. Fontes, D.H. Sampson, H.L. Zhang, Phys. Rev. A 48 (1993) 1975.
35. S.M. Younger, Phys. Rev. A 22 (1980) 111.
36. K. Aichele, and U. Hertenfeller, J. Phys. B 31 (1998) 2369.
37. E.D. Donets, V.P. Ovsyannikov, Sov. Phys. JETP 53 (1981) 466.
38. J.A. Kunc, J. Phys. B 13 (1980) 587.
39. X.H. Shi, C.Y. Chen, Y. Zhao, Y.S. Wang, J. Quant. Spectrosc. Radiat. Transfer 91 (2005) 161.
40. R.E. Marrs, S.R. Elliott, J.H. Scofield, Phys. Rev. Lett. 72 (1994) 4082.
41. B. O'Rourke, F.J. Currell, H. Kuramoto, Y.M. Li, S. Ohtani, X.M. Tong et al., J. Phys. B 34 (2002) 4003.
42. H. Watanabe, F.J. Currell, H. Kuramoto, S. Ohtani, B. O'Rourke, X.M. Tong, J. Phys. B 35 (2002) 5095.
43. D.L. Moores, K.J. Reed, Phys. Rev. A 51 (1995) R9.
44. R.E. Marrs, S.R. Elliott, D.A. Knapp, Phys. Rev. Lett. 72 (1994) 4082.

APPENDICES

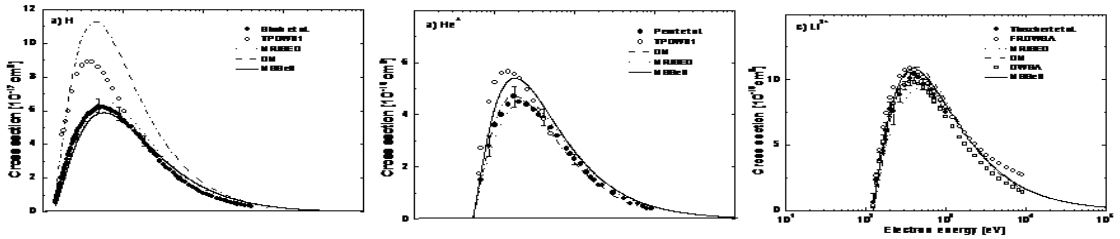

Figure 1: Electron Impact Ionization Cross Sections of *H*-like Targets: a) H, b) He^{1+}, and c) Li^{2+}

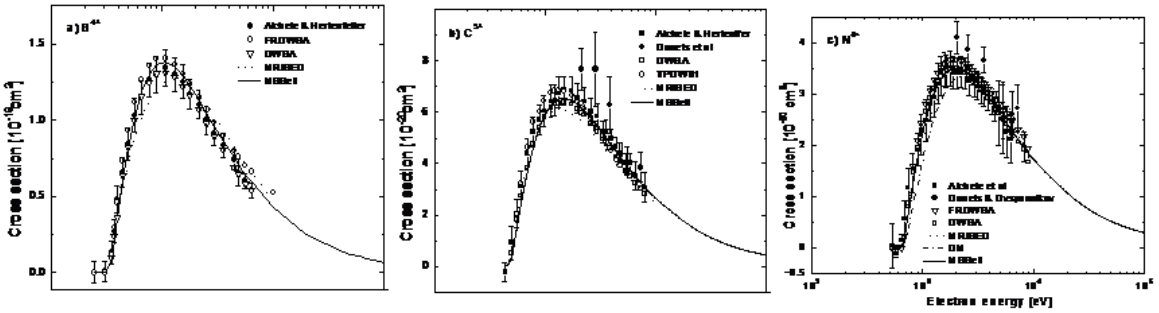

Figure 2: Same as in Figure 1 for: a) $B^{4+,}$ b) C^{5+}, and c) N^{6+}

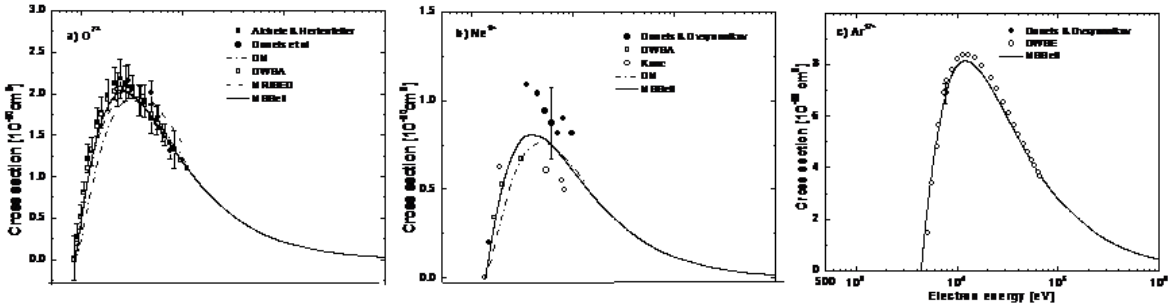

Figure 3: Same as in Figure 1 for: a) O^{7+}, b) Ne^{9+}, and c) Ar^{17+}

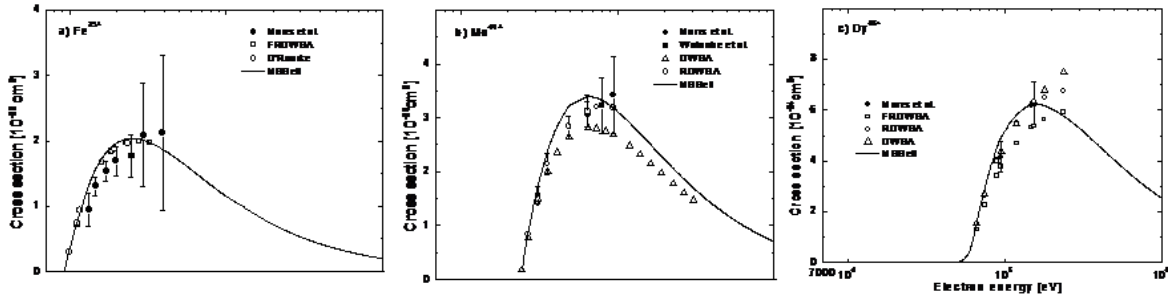

Figure 4: Same as in Figure 1 for: a) Fe^{25+}, b) Mo^{41+}, and c) Dy^{65+}

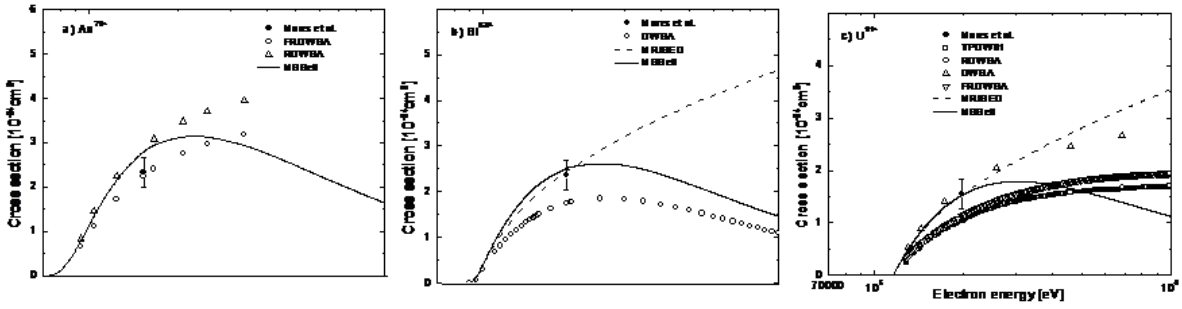

Figure 5: Same as in Figure 1 for: a) Au^{78+}, b) Bi^{82+}, and c) U^{91+}